Micro-Raman Scattering From Hexagonal GaN, AlN, and $Al_xGa_{1-x}N$ Grown on (111) Oriented Silicon: Stress Mapping of Cracks

C. Ramkumar, T. Prokofyeva, M. Seon,[1] and M. Holtz
Department of Physics and NanoTech Center, Texas Tech University,
Lubbock, TX 79409, U.S.A.
K. Choi, J. Yun, S. A. Nikishin, and H. Temkin
Department of Electrical Engineering and NanoTech Center, Texas Tech University,
Lubbock, TX 79409, U.S.A.
[1]Samsung Advanced Technology, Samsung Corporation,
P.O. Box 111, Suwon 440-600, South Korea.

ABSTRACT

We report post-growth micro-Raman stress mapping of cracks in GaN, AlN, and $Al_xGa_{1-x}N$ grown on (111) oriented silicon. Cracks with an average spacing of ~ 100 μm are observed. These cracks are categorized into two types. The first type of crack propagates through the epilayer, and several microns deep into the substrate and is observed in all the samples investigated. The second type cracks epilayer only and is observed only in GaN. The micro-Raman stress mapping of the first type of crack shows that the epilayers are under biaxial tensile (< 0) stress and the silicon substrate is under compressive (> 0) stress far away from the cracks. The stress in the epilayers as well the substrate is found to relax from the equilibrium (far away from the cracks) value of –0.5 GPa (AlN), -0.16 GPa (GaN), -0.6 GPa ($Al_xGa_{1-x}N$) and 0.36 GPa (Si) as the crack position is approached. Partial relaxation is observed to occur over a range of 10 μm. At the crack position, the epilayers and the substrate are relaxed to nearly zero stress values. The stress mapping of the second type of crack reveals that the substrate is completely relaxed (stress is close o zero) far away from the cracks. At the crack position the GaN epilayer is partially relaxed from –0.2 GPa to –0.08 GPa, while the silicon substrate is seen to be under tensile stress of –0.39 GPa. The stress map of epilayers is well described by the distributed force model for both types of cracks. Furthermore, the calculated stress profiles of cracked and uncracked substrate using the above mentioned model are in excellent agreement with the experimental data.

INTRODUCTION

Semiconducting and hexagonal phase AlN, GaN, and $Al_xGa_{1-x}N$ alloys have received a great deal of interest [1] because of their potential optoelectronic and electronic device applications. These systems offer energy gaps ranging from 3.4 to 6.3 eV. Generally, these materials are grown on non-ideal substrates like sapphire, silicon carbide, or silicon using epitaxial methods. However, the epilayers exhibit large stresses due to mismatches in both the lattice constants and the thermal expansion coefficients of the nitride semiconductors and the substrate. The presence of large stresses [2,3] can promote crack generation and propagation, which are detrimental to device fabrication. The problem of cracking has been overcome by initially depositing an AlN epilayer and the reproducible growth of these materials on (111)-oriented silicon substrates *without any cracking* has been demonstrated [4,5]. Similar results have been recently reported for GaN grown on Si substrates [6]. Nevertheless, cracks in nitrides remain a persistent and

interesting problem to be investigated. Several studies have aimed at understanding stress-induced cracking [7-9]. These studies have mainly focused on global stresses in GaN and AlGaN deposited on sapphire, with the exception of one micro-Raman stress mapping study [8]. In Ref. [8], the authors investigated cracks in the GaN epilayer only and did not address stress in the substrate. In this paper, we present post-growth stress mapping of cracks in GaN, AlN, and $Al_xGa_{1-x}N$ deposited on (111) oriented silicon. We report the first micro-Raman study of cracks in III-nitride layers grown on silicon substrates, which addresses simultaneously the stress in the epilayer and in the substrate. We find that the stress map in both epilayer and substrate are well described using the distributed force model [10,11] in all cases.

EXPERIMENTAL DETAILS

Epilayers of AlN, GaN, and $Al_xGa_{1-x}N$ ($x = 0.35$) were grown on Si (111) substrates by gas-source molecular beam epitaxy using ammonia as the nitrogen source and effusion cells for the metals. The substrate temperature was kept between 1100 and 1160 K during deposition. For GaN and $Al_xGa_{1-x}N$, an AlN buffer layer (≈ 50 nm thick) was first grown. Total thicknesses were 1.25 μm (GaN), 0.76 μm ($Al_xGa_{1-x}N$), and 0.80 μm (AlN) from scanning electron microscopy (SEM) and reflectance measurements. The alloy composition was found by reflectance and electron-probe microanalysis. Cracks were produced in the epilayers by rapid deposition followed by rapid cooling from the growth temperature to ambient. The cracks are known to form along $\{1\bar{1}00\}$ lattice planes [12]. They are spaced somewhat regularly, with typical separation ≈ 100 μm. In spite of the cracks, the epilayers showed excellent adhesion to the substrate. Stress maps were obtained using a micro-Raman instrument with a high-resolution (0.2 μm) translation stage and 488-nm laser excitation focused to a spot diameter between 1 and 2 μm [13]. The stress measurement accuracy is ≈ 0.05 GPa for silicon and ≈ 0.01 GPa for epilayers.

RESULTS AND DISCUSSION

Raman scattering has been used extensively for determining stress in epitaxial GaN [13,14]. This is accomplished by measuring the E_2^2-phonon energy in stressed and unstressed GaN, and by using the associated Raman-stress factor, $\partial\omega/\partial\sigma$, where σ is biaxial stress perpendicular to the growth axis. Values reported in the literature for the Raman stress factor of GaN vary. We use here the result of Lee, *et al.* –7.7 cm^{-1}/GPa [15]. For AlN, we use –6.3 cm^{-1}/GPa [3]. There is no corresponding data for $\partial\omega/\partial\sigma$ in $Al_xGa_{1-x}N$ alloys, but it is reasonable to expect it to be close to that of GaN and AlN. Based on this, it is possible to convert the phonon energy shift to stress, assuming it is biaxial. At and in the neighborhood of the crack, the so-called shear-lag zone, the stress tensor evolves from biaxial to one having $\sigma_{1'1'}$, $\sigma_{1'3}$, and σ_{33} terms [10,11]. Here, $1'$ corresponds to the axis perpendicular to the crack plane and 3 is along the direction of the growth axis. In order to properly use these stresses to determine the associated Raman frequency shifts, as is done in [16] for silicon, the six piezospectroscopic coefficients for the hexagonal nitrides are required. Since these have not yet been reported, we apply the biaxial analysis in order to estimate the stress from the frequency shift. Moreover, the stress is collapsing across the shear-lag zone, any effect due to the $\sigma_{1'3}$, and σ_{33} (and $\sigma_{1'1'}$) tensor terms also diminishes. Therefore, we approximate the stress using the $\sigma_{1'1'}$ component only, knowing that all the other stress components are tending to zero.

Figure 1(a) shows the SEM picture of type 1 crack. The cracking results in a crevice approximately 25 nm wide. SEM images of numerous cracks show that the crack has propagated ≈ 2-4 μm into the substrate along {110} lattice planes. Figure 1(b) shows an SEM cross-section of type 2 crack in the GaN layer, which has not propagated into the substrate. Figure 2(a) shows a line image of the shift in the E_2^2-phonon energy vs. position across type 1 cracks in each of the samples studied. The right-hand scale of Fig. 2 shows the stress using the AlN stress factor. Far from the crack positions, the E_2^2-phonons of AlN and GaN shift by about –3.0 and -1.2 cm^{-1} respectively, implying a (tensile) stress of ≈ -0.5 and -0.16 GPa. Tensile stress due to thermal expansion mismatches between AlN and GaN, and the silicon substrate, are estimated to be ≈ -0.6 GPa [3] and -0.39 GPa [13], respectively. The reduced stress values obtained from the Raman measurements indicate that the epilayers are partially relaxed because of high-density crack formation. The tensile stress in the AlN and GaN samples is seen to relax at the position of the crack (defined as the origin). The solid curves shown are calculated stress profiles using the model of Ref. [10,11]. The model describes the stress relaxation profile, using the stress value far from the crack (not shown) of ≈ -0.50 GPa (AlN) and -0.16 GPa (GaN) as model parameters. The other model parameters are the measured layer thickness, which gives the width of the relaxation in Fig. 1, and the elastic moduli of AlN [17] and GaN [17], and silicon [18].

The stress map for a crack in the *x*=0.35 alloy is also shown in Fig. 2(a). The large shift seen at the crack in the GaN-like E_2^2-phonon, comparable to what is seen in our GaN and AlN, suggests that the alloy also relaxes at this position. The Raman stress factor will depend on composition. We assume that the alloy will have an E_2^2 phonon stress factor close to that of the endpoint materials. The right-hand scale for stress in AlN thus serves as an approximate scale for $Al_xGa_{1-x}N$. The red shift observed in the alloy sample, far from the crack, is ≈ -3.5 cm^{-1}, corresponding to an approximate (tensile) biaxial stress of –0.6 GPa. The model calculation shown also describes the map of stress relaxation for the alloy quite well. In all cases, agreement between the data and the model is excellent.

In addition to a stress map from the epilayers, we also obtain the position dependence of the silicon substrate phonon energy. The dependence is shown in Fig. 2(b) for the GaN sample. The corresponding dependence for the AlN and alloy samples was comparable. Close to the crack, we observe the dependence expected from applying the model calculation of Ref. [11] to the *substrate*. We have used the biaxial stress term to obtain the stress from the Raman frequency shift even though the three terms of the piezospectroscopic tensor are known [19]. This is because the position dependence of σ_{13} term does not agree with the measured position dependence of silicon phonon energy and the σ_{33} term is one order magnitude smaller than the σ_{11} component. The stress is found to vary rapidly from point to point (on the micron scale) directly under the crack and a partial relaxation is observed over ≈ 10 μm range, which is much larger than our probe size (1-2 μm). We see a stress relaxation at the position of the crack, suggesting that the *silicon* has also cracked with the nitride layers. The suggestion that the epilayer stress has released so energetically that the substrate has cracked is confirmed in Fig. 1(a). It is interesting to note that the adhesion between the substrate and epilayer is sufficiently strong to remain intact despite the evident ferocity of the cracking process.

Far from the crack (> 10 μm), we determine the stress in the silicon (GaN sample) to be compressive with a value of ≈ 0.36 GPa, using the Raman stress factor in Ref. [16]. This value is

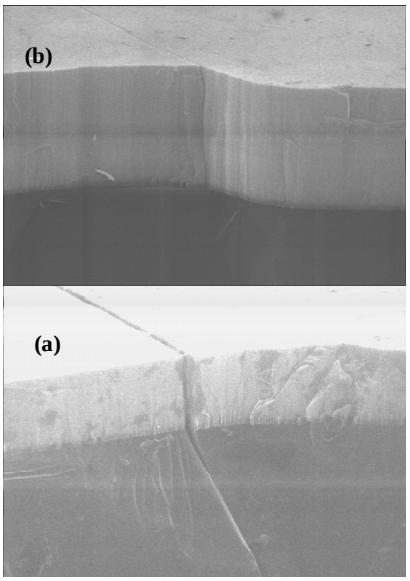

Figure 1(a). Cross sectional scanning electron microscope picture of first type of crack. (b) The same for second type of crack.

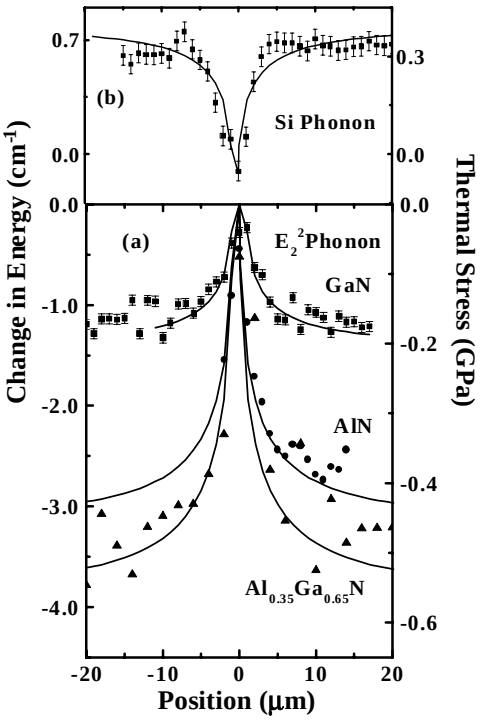

Figure 2(a). Line Image of E_2^2 phonon energy shift of GaN (■), AlN (●)and $Al_{0.35}Ga_{0.65}N$ (▲) vs. position across first type of crack. (b) Line image of LO Phonon energy shift of silicon substrate for the same type of crack. Solid lines represent calculated stress profiles using distributed force model.

found to be larger than the tensile stress in the GaN (-0.16 GPa). However, the compressive stress in the silicon in AlN and $Al_xGa_{1-x}N$ samples is found to have the same magnitude as the tensile stress in the epilayers. Our SEM measurements on all three samples show that all cracks studied in AlN and $Al_xGa_{1-x}N$ epilayers propagated into the substrate. In GaN, only a few cracks propagated into the substrate, allowing a lesser degree of stress relaxation. Therefore, the discrepancy in the magnitude is attributed to the low density of crack formation in the silicon substrate. Raman measurements on type 2 crack in GaN indicate that the epilayers are under tensile stress (0.34 GPa) far away from the crack. This stress is entirely due to the thermal expansion coefficient mismatch [13]. The substrate is found be in a stress-free state due to its large relative thickness. In contrast, for type 1 crack, the substrate is found to be under compressive stress far away from the crack. The compressive stress in the substrate is measurable because the cracking creates monolithic domains with a relatively small area and an effective thickness, which corresponds to the crack depth. This small effective size allows the substrate to relax under the tensile stress of the epilayer for type 2 crack.

The Raman stress map for the type 2 crack is shown in Fig. 3(a). The GaN does not appear to completely relax at the position of this crack. This is possibly due to the fact that this crack has not resulted in an open fissure and tensile stress remains due to the substrate. What is interesting is that the stress map in the substrate Fig. 3(b) is very different from what we saw in Fig. 2(b). In this case, the stress is close to zero far from the crack, gradually grows compressive and becomes

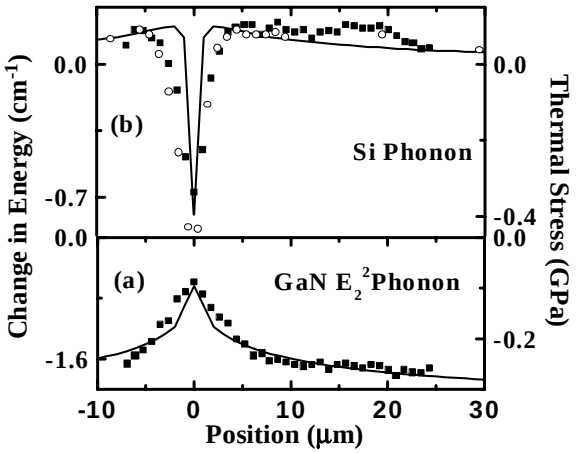

Figure 3. Line image of (a) E_2^2 phonon energy shift of GaN (■) and (b) LO phonon energy shift of silicon (■ and ○) substrate vs. position across second type of crack. Solid lines represent the distributed force model description of experimental data.

tensile near the crack. The tensile stress at the crack is attributed to contraction in the nitride layers on each side of the crack-tip. The compressive stress close to the crack is due to contraction in the silicon slabs (domains) close to the crack. This behavior is predicted by the stress model [10,11], which allows us to calculate the stress in the substrate under the type 2 crack in the epilayer. However, the stress in the silicon is depth dependent. Since the silicon attenuates the Raman excitation and scatter, we calculate the weighted average using

$$\langle \sigma_{\perp} \rangle = \frac{1}{d_{opt}} \int_0^{\infty} \sigma_{\perp}(z) e^{-z/d_{opt}} dz \qquad (1)$$

where z is depth into the silicon from the interface and $d_{opt} = 1/2\alpha$ is the optical penetration depth of the laser light into the silicon (≈ 0.4 μm). The calculated result is shown in Fig. 3(b) for $\langle \sigma_{\perp} \rangle$. Outside of d_{opt}, we introduce no new parameters in this calculation beyond what was used for modeling the stress in the epilayer.

CONCLUSIONS

We present a comprehensive stress mapping study of cracks in GaN, AlN, and $Al_xGa_{1-x}N$, as well as silicon substrate. Generally, the epilayer is observed to be under tensile stress and the substrate is under compressive stress. Two types of cracks are investigated (Fig. 1). The first type of crack propagates vertically through the entire epilayer thickness and several microns into the substrate. The second type cracks the epilayer but does not propagate into the substrate. Only the first type of crack is observed in the AlN and $Al_xGa_{1-x}N$, for which the stress relaxes at the point of the crack and shows partial relaxation over ≈ 10 μm range (Fig. 2). We examine both types of cracks in GaN. In the second crack type, the stress in the epilayer partially relaxes at the crack position, and we see the stress in the substrate to be *tensile* at this position (Fig. 3). The epilayer stress map is well described by the analytical model of Refs. [10,11] for both types of cracks. Furthermore, the calculated stress profiles of cracked and uncracked substrates are in excellent agreement with our data.

ACKNOWLEDGEMENTS

The authors wish to thank J. Hashemi for helpful discussions. Support for this work is acknowledged from the State of Texas Advanced Technology Program, the National Science Foundation (ECS0070240 and DMR-9705498), DARPA (F19628-99-0013) and CRDF (RE-2217).

REFERENCES

1. S. J. Pearton, J. C. Zolper, R. J. Shul, and F. Ren, J. Appl. Phys. **86**, 1 (1999).
2. C. Kisielowski, J. Krüger, S. Ruvimov, T. Suski, J. W. Ager, E. Jones, Z. Liliental Weber, M. Rubin, E. R. Weber, M. D. Bremser, and R. F. Davis, Phys. Rev. B **54**, 17745 (1996).
3. T. Prokofyeva, M. Seon, J. Vanbuskirk, M. Holtz, S. A. Nikishin, N. N. Faleev, H. Temkin, and S. Zollner, Phys. Rev. B **63**, 125313 (2001).
4. S. A. Nikishin, N. N. Faleev, V. G. Antipov, S. Francoeur, L. Grave de Peralta, G. A. Seryogin, H. Temkin, T. I. Prokofyeva, M. Holtz, and S. N. G. Chu, Appl. Phys. Lett. **75**, 2073 (1999).
5. S. A. Nikishin, V. G. Antipov, S. Francoeur, N. N. Faleev, G. A. Seryogin, V. A. Elyukhin, H. Temkin, T. I. Prokofyeva, M. Holtz, A. Konkar, and S. Zollner, Appl. Phys. Lett. **75**, 484 (1999).
6. F. Semond, P. Lorenzini, N. Grandjean, and J. Massies, Appl. Phys. Lett. **78**, 335 (2001).
7. S. J. Hearne, J. Han, S. R. Lee, J. A. Floro, D. M. Foolstaedt, E. Chason, and I. S. T. Tsong, Appl. Phys. Lett. **76**, 1534 (2000).
8. L. T. Romano, C. G. Van de Walle, J. W. Ager, W. Götz, and R. S. Kern, J. Appl. Phys. **87**, 7745 (2000).
9. E. V. Etzkorn and D. R. Clarke, J. Appl. Phys. **89**, 1025 (2001).
10. S. M. Hu, J. Appl. Phys. **50**, 4661 (1979).
11. A. Atkinson, T. Johnson, A. H. Harker, and S. C. Jain, Thin Solid Films **274**, 106 (1996).
12. D. M. Follstaedt, J. Han, P. Provencio, and J. G. Fleming, MRS Internet J. Nitride Semicond. Res. **4S1**, G3.72 (1999).
13. M. Seon, T. Prokofyeva, M. Holtz, S. A. Nikishin, N. N. Faleev, and H. Temkin, Appl. Phys. Lett. **76**, 1842 (2000).
14. H. Siegle, P. Thurian, L. Eckey, A. Hoffmann, C. Thomsen, B. K. Meyer, H. Amano, I. Akasaki, T. Detchprohm, and K. Hiramatsu, Appl. Phys. Lett. **68**, 1265 (1996).
15. I. H. Lee, I. H. Choi, C. R. Lee, E. J. Shin, D. Kim, S. K. Noh, S. J. Son, K. Y. Lim, and H. J. Lee, J. Appl. Phys. **83**, 5787 (1998).
16. I. De Wolf, J. Vanhellemont, A. Romano-Rodríguez, H. Norström, and H. E. Maes, J. Appl. Phys. **71**, 898 (1992).
17. V. Yu. Davydov, Yu. E. Kitaev, I. N. Goncharuk, A. N. Smirnov, J. Graul, O. Semchinova, D. Uffmann, M. B. Smirnov, A. P. Mirgorodsky, and R. A. Evarestov, Phys. Rev. B **58**, 12899 (1998).
18. D. Gerlich, S. L. Dole, and A. Slack, J. Phys. Chem. Solids **47**, 437 (1986).
19. E. Anastassakis, A. Cantarero, and M. Cardona, Phys. Rev. B **41**, 7529 (1990).